ORIGINAL ARTICLE

OPEN ACCESS

Hyaluronan impairs vascular function and drug delivery in a mouse model of pancreatic cancer

Michael A Jacobetz,[1] Derek S Chan,[1,2] Albrecht Neesse,[1] Tashinga E Bapiro,[1,2] Natalie Cook,[1,2] Kristopher K Frese,[1] Christine Feig,[1] Tomoaki Nakagawa,[1] Meredith E Caldwell,[1] Heather I Zecchini,[1] Martijn P Lolkema,[1] Ping Jiang,[3] Anne Kultti,[3] Curtis B Thompson,[3] Daniel C Maneval,[3] Duncan I Jodrell,[1] Gregory I Frost,[3] H M Shepard,[3] Jeremy N Skepper,[4] David A Tuveson[1,2]

► Additional materials are published online only. To view these files please visit the journal online (http://dx.doi.org/10.1136/gutjnl-2012-302529).

[1]Cancer Research UK Cambridge Research Institute, Cambridge, UK
[2]Department of Oncology, Cambridge University Hospitals NHS Foundation Trust, Cambridge, UK
[3]Halozyme Therapeutics, Inc., San Diego, California, USA
[4]Multi-Imaging Centre, Physiology Development and Neuroscience, University of Cambridge, Cambridge, UK

Correspondence to
Dr David Tuveson, Cancer Research UK Cambridge Research Institute, Li Ka Shing Centre, Cambridge CB2 0RE, UK; david.tuveson@cancer.org.uk

DSC and AN contributed equally to this work.

Accepted 19 March 2012
Published Online First 30 March 2012

ABSTRACT

Objective Pancreatic ductal adenocarcinoma (PDA) is characterised by stromal desmoplasia and vascular dysfunction, which critically impair drug delivery. This study examines the role of an abundant extracellular matrix component, the megadalton glycosaminoglycan hyaluronan (HA), as a novel therapeutic target in PDA.

Methods Using a genetically engineered mouse model of PDA, the authors enzymatically depleted HA by a clinically formulated PEGylated human recombinant PH20 hyaluronidase (PEGPH20) and examined tumour perfusion, vascular permeability and drug delivery. The preclinical utility of PEGPH20 in combination with gemcitabine was assessed by short-term and survival studies.

Results PEGPH20 rapidly and sustainably depleted HA, inducing the re-expansion of PDA blood vessels and increasing the intratumoral delivery of two chemotherapeutic agents, doxorubicin and gemcitabine. Moreover, PEGPH20 triggered fenestrations and interendothelial junctional gaps in PDA tumour endothelia and promoted a tumour-specific increase in macromolecular permeability. Finally, combination therapy with PEGPH20 and gemcitabine led to inhibition of PDA tumour growth and prolonged survival over gemcitabine monotherapy, suggesting immediate clinical utility.

Conclusions The authors demonstrate that HA impedes the intratumoral vasculature in PDA and propose that its enzymatic depletion be explored as a means to improve drug delivery and response in patients with pancreatic cancer.

Significance of this study

What is already known on this subject?

- The tumour microenvironment in PDA is characterised by hypovascularity and extensive deposits of extracellular matrix components.
- The desmoplastic and hypovascular nature of PDA contributes to its unique therapeutic resistance in part by impairing efficient drug delivery.

What are the new findings?

- HA is a non-sulphated glycosaminoglycan that is highly abundant in the extracellular matrix of human and murine PDA.
- Enzymatic depletion of HA by PEGPH20 induced the re-expansion of PDA blood vessels and increased the delivery of two chemotherapeutic agents in a genetically engineered mouse model of PDA.
- PEGPH20 promoted a tumour-specific increase in macromolecular permeability and induced fenestrations and interendothelial junctional gaps in PDA endothelia.
- Combination therapy with PEGPH20 and gemcitabine inhibits tumour growth and prolongs survival in a genetically engineered mouse model of PDA.

How might it impact on clinical practice in the foreseeable future?

- Increasing drug delivery to hypovascular and stroma-rich tumours is a promising strategy to circumvent therapeutic resistance in PDA. HA is an attractive target in the tumour microenvironment of PDA.
- The synergism of PEGPH20 and gemcitabine is of immediate clinical significance and provides support for investigational trials with this therapeutic combination.

INTRODUCTION

Pancreatic ductal adenocarcinoma (PDA) is a malignancy with a dire prognosis due to aggressive disease on clinical presentation and poor chemotherapeutic response.[1] The fluorinated nucleoside analogue gemcitabine (2′,2′-difluorodeoxycytidine, dFdC) remains the antineoplastic agent of choice, offering a survival benefit of little more than 5 weeks,[2] while gemcitabine-based combination therapies have shown limited progress in advancing survival.[3]

Understanding of genetic alterations in PDA has allowed the generation of genetically engineered mouse models (GEMMs), bearing autochthonous tumours that recapitulate the human pathology.[4–6] A mechanism for intrinsic gemcitabine resistance has recently been reported in one such GEMM, the *LSL-Kras$^{G12D/+}$;LSL-Trp53$^{R172H/+}$;Pdx-1-Cre* (KPC) mouse.[7] Compared with subcutaneous tumours of syngeneic origin, KPC tumours demonstrated a desmoplastic stroma and lower mean vessel densities, thus limiting the accumulation of the active gemcitabine triphosphate (dFdCTP).[7] A similar perfusion deficit has been observed in an

Table 1 Human TMA

Tissue origin	% Cases with +HA staining
Breast	Tumour (N=117, 56%)
	Normal (N=13, 23%)
Prostate	Tumour (N=110, 46%)
	Normal (N=17, 5.8%)
Bladder	Tumour (TCC) (N=106, 43%)
	Normal (N=8, 0%)
Stomach	Tumour (adenocarcinoma) (N=95, 42%)
	Normal (N=14, 0%)
Pleura	Tumour (mesothelioma) (N=52, 37%)
	Normal (N=15, 0%)
Lung	NSCLC (N=169, 29%)
	SCLC (N=21, 10%)
	Normal (N=21, 0%)
Ovary	Tumour (N=185, 12%)
	Normal (N=31, 0%)
Colon	Tumour (N=136, 28%)
	Normal (N=25, 8%)
Bone marrow	Multiple myeloma (N=27, 3.7%)
	Normal (N=35, 0%)
Pancreas	Ductal adenocarcinoma (N=99, 90%)
	Acinar cell carcinoma (N=2, 0%)
	Mucinous adenocarcinoma (N=5, 100%)
	Papillary adenocarcinoma (N=4, 25%)
	Squamous cell carcinoma (N=2, 100%)
	Normal (N=25, 4%)

HA staining is most common in pancreatic ductal adenocarcinoma in comparison to other major human tumours.
HA, hyaluronan. TMA, tissue microarray. TCC, transitional cell carcinoma. NSCLC, non-small cell lung carcinoma. SCLC, small cell lung carcinoma.

independent study in mice and human PDA.[8 9] Stromal depletion by Smoothened inhibition in KPC mice increased perfusion, intratumoral dFdCTP and overall survival, suggesting that therapeutic failure of gemcitabine arises from a potentially reversible impairment in drug delivery.[7]

Of note, the scarcity of tumour vessels is compounded by a vessel perfusion mismatch,[7 8] which is likely a result of interstitial hypertension and vascular compression.[10–12] Vascular hyperpermeability, water retention by extracellular matrix components and inadequate lymphatic drainage contribute towards interstitial fluid pressure (IFP) in solid tumours, and its selective decrease in malignant tissues represents an approach in maximising the delivery and hence the therapeutic indices of chemotherapeutic agents.[13] Indeed, the IFP reduction associated with vascular endothelial growth factor (VEGF) inhibitors is likely central to their clinically beneficial synergism with cytotoxic agents.[14]

Hyaluronan (HA) is a non-sulphated glycosaminoglycan present in the extracellular matrix, composed of N-acetylglucosamine/glucuronic acid disaccharide repeats of variable length. HA may signal through 'hyaladherins' such as CD44 to regulate receptor tyrosine kinase and small GTPase activity and is implicated in the processes of angiogenesis, epithelial–mesenchymal transition and chemoresistance.[15] Moreover, HA's anionic repeats also sequester mobile cations and solvating water, resulting in osmotic swelling that provides structural support in HA-rich normal and malignant tissues.[16] Degradation of HA by intratumoral administration of bovine hyaluronidases showed promise in diminishing tumorous IFP and increasing chemotherapeutic index in xenograft models,[17 18] but systemic administration was limited by short residence time and immunogenicity.[19] PEGPH20, a PEGylated human recombinant PH20 hyaluronidase, surmounts these issues and has demonstrated comparable activity in vivo, inducing rapid perfusion increase in xenograft tumours.[20]

HA is a known secretory product of several human pancreatic carcinoma cell lines[21] and has been shown as an over-represented glycosaminoglycan in human PDA,[22] localised to the stroma and peritumoral connective tissue.[23] However, in contrast to other epithelial cancers, the pathological significance of its rheological and signalling properties has not been fully investigated in this malignancy.[24] In this study, we sought to investigate the aetiology of vascular compression in the KPC GEMM and identified HA as a critical modifier of tumorous vascular function. Its enzymatic depletion by PEGPH20 resulted in an improvement in tumour vascular patency, as well as an unexpected selective change in tumour endothelial ultrastructure and macromolecular permeability. Our data predict hyaluronidase synergism with cytotoxic agents and demonstrate a significant survival benefit with combination therapy, providing HA as a novel stromal therapeutic target to consider for patients with pancreatic cancer.

MATERIALS AND METHODS

Mice

Experiments were carried out within the Cancer Research UK Cambridge Research Institute's Biological Resources Unit, under the terms of the Home Office Project Licenses PPL80/2072 and 80/2539 and subject to Cancer Research UK ethical review. The generation of tumour-bearing KPC (*LSL-Kras$^{G12D/+}$;LSL-Trp53$^{R172H/+}$;Pdx-1-Cre*) mice has previously been described.[5] Where appropriate, PC (*LSL-Trp53$^{R172H/+}$;Pdx-1-Cre*) littermates, which did not develop any pancreatic lesions within the experimental time frame, served as healthy controls. KPC mice were enrolled onto studies once tumour volume reached 270±100 mm^3, as assessed by three-dimensional ultrasonography.[7]

Vascular function studies

At least four mice were evaluated for each experimental arm. One hour after the final dose of PEGPH20, mice received an intravenous infusion of fluorophore-labelled lectin only (vascular patency assay) or of fluorophore-labelled lectin and dextrans (permeability assay). Thirty minutes later, mice were terminally perfused with 30 ml of 4% paraformaldehyde/phosphate buffered saline (pH 7.4). Perfused tissues were harvested, fixed for 16–24 h in paraformaldehyde and transferred to 70% ethanol before paraffin embedding. Sections were deparaffinised, rehydrated and, for vascular patency assays, immunostained for MECA-32 (see Immunostaining and HA histochemistry section). All sections were counterstained with 4′,6-diamidino-2-phenylindole (DAPI). Visualisation was performed on a Leica SP5 confocal microscope (Leica Microsystems, Wetzlar, Germany) using standardised settings, and background signal intensities were established against unlabelled terminally perfused samples. Mean vessel densities were quantified as the average number of CD31$^+$ vessels in a minimum of 10 non-adjacent 40× fields.

Pharmacodelivery studies

For the doxorubicin delivery assay, a minimum of five mice from each arm were included for analysis. Mice received an intravenous infusion of doxorubicin 1 h after the final dose of PEGPH20. Mice were then terminally perfused with paraformaldehyde, and tissues processed as above. Sections were deparaffinised, rehydrated and counterstained with DAPI. Doxorubicin fluorescence was quantified with the CompuCyte iCys Research Imaging Cytometer and iNovator software (CompuCyte Westwood, MA, USA), as previously described.[7]

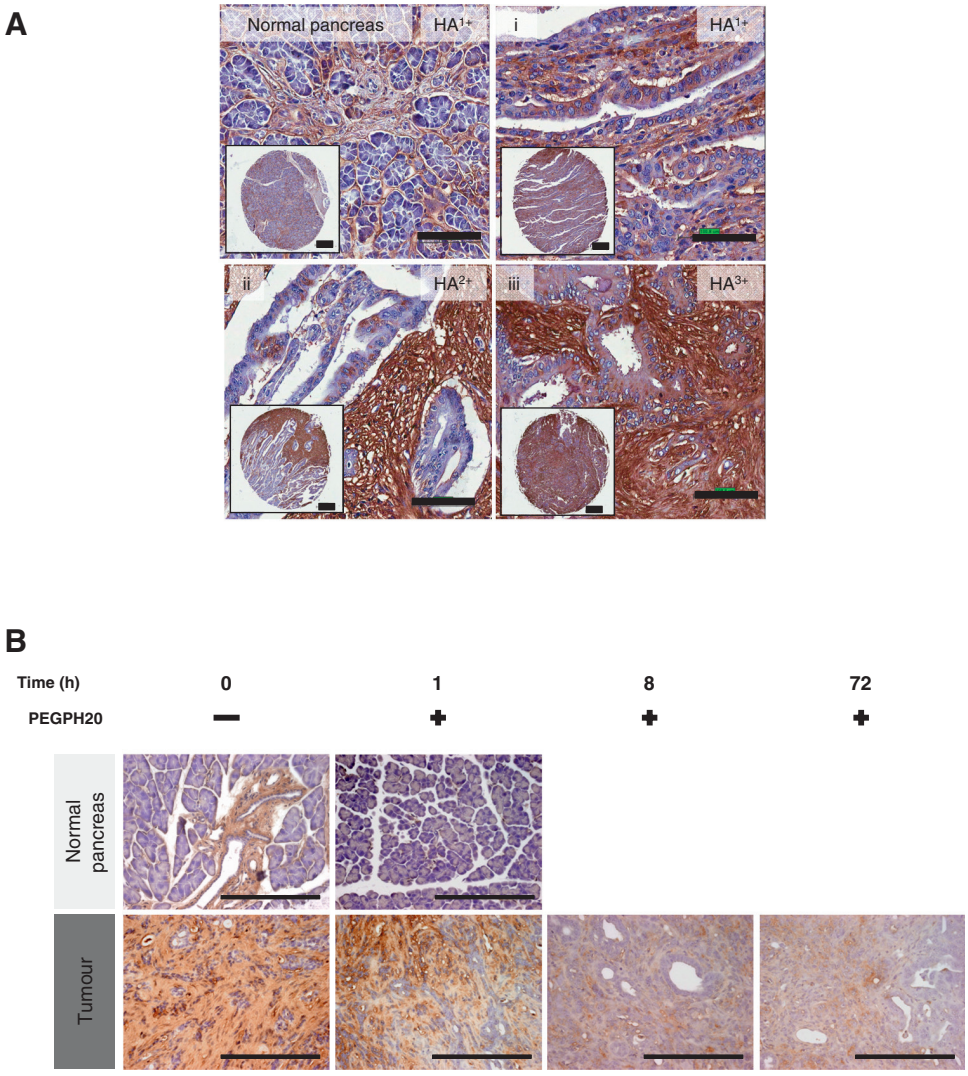

Figure 1 Hyaluronan (HA) accumulates in pancreatic ductal adenocarcinoma (PDA) and may be rapidly and sustainably degraded by PEGPH20. (A) HA expression in human pancreatic cancer samples (i–iii) varies from low expression (HA^{1+}) to high expression (HA^{3+}), with little HA detected in normal pancreas (top left panel) (scale bar: inset 300 μm, 100 μm). (B) HA expression in normal pancreas and PDA over time after treatment with PEGPH20. PEGPH20 treatment specifically degrades HA in normal pancreas (top row) 1 h after treatment. Maximal HA degradation was achieved in KPC tumours 8 h after PEGPH20 treatment that still remained low even 72 h after treatment. n=3 mice per time point (scale bar: 200 μm).

For the gemcitabine delivery assay, a minimum of five mice from each arm were included for analysis. Mice received intravenous gemcitabine 8 h after a single dose of PEGPH20 or vehicle. Plasma was obtained by cardiac puncture under terminal isoflurane anaesthesia, 2 h after gemcitabine administration, and tissues were harvested shortly thereafter. All samples were frozen in liquid nitrogen and processed as described for liquid chromatography-tandem mass spectrometry analysis of fluorinated metabolites.[25]

Survival study

KPC mice bearing tumours of 270±100 mm^3 were assigned to one of four arms—vehicle, intraperitoneal gemcitabine, PEGPH20 or PEGPH20/intraperitoneal gemcitabine in combination (dosed 30 min apart)—and treatments were administered accordingly. Once enrolled onto a survival study, mice were monitored by three-dimensional ultrasonography every 3 days to allow calculation of tumour volumes. Endpoint criteria were defined as 20% body weight loss in addition to general morbidity, lethargy, lack of social interaction or development of ascites.

Immunostaining and HA histochemistry

Samples at study end point were fixed in 4% paraformaldehyde or in 10% neutral buffered formalin for 16–24 h and transferred to 70% ethanol before paraffin embedding. Three-micrometre sections were generated, and one section from each sample was stained with H&E for analysis of morphological integrity. Where appropriate, stained sections were scanned at 20× magnification using Aperio ScanScope CS instrument and were analysed in Spectrum (Aperio Vista, CA, USA).

For immunostaining with most antibodies, sections were deparaffinised, rehydrated and antigen retrieval performed with citric acid (pH 6.0) in an 850 W microwave. For CD31 immunostaining, antigen retrieval was performed with proteinase K at 37°C. Non-specific protein binding was blocked with 10% goat serum (Sigma St Louis, MA, USA) for immunohistochemistry and 10% donkey serum (Sigma) for immunofluorescence. Sections were incubated with primary antibodies for 1 h at room temperature or overnight at 4°C. The primary antibodies used were against PV-1 (MECA-32, 1:50; Santa Cruz Biotechnology, Santa Cruz, CA, USA) and CD31 (MEC 13.3, 1:50; BD Biosciences, Franklin Lakes, NJ, USA). For immunohistochemistry, remaining steps were carried out using appropriate Vectastain Elite ABC kits (Vector Laboratories, Burlingame, CA, USA) and DAB Peroxidase Substrate (Vector Laboratories), with haematoxylin counterstaining. For immunofluorescence, sections were incubated with appropriate AlexaFluor-conjugated secondary antibodies for 1 h at room temperature and counterstained with DAPI.

For HA histochemistry, biotinylated HA binding protein (bHABP, Calbiochem catalogue number 385911; Merck KGaA, Darmstadt, Germany) was used. Sections were deparaffinised, rehydrated and blocked with 3% bovine serum albumin (BSA)

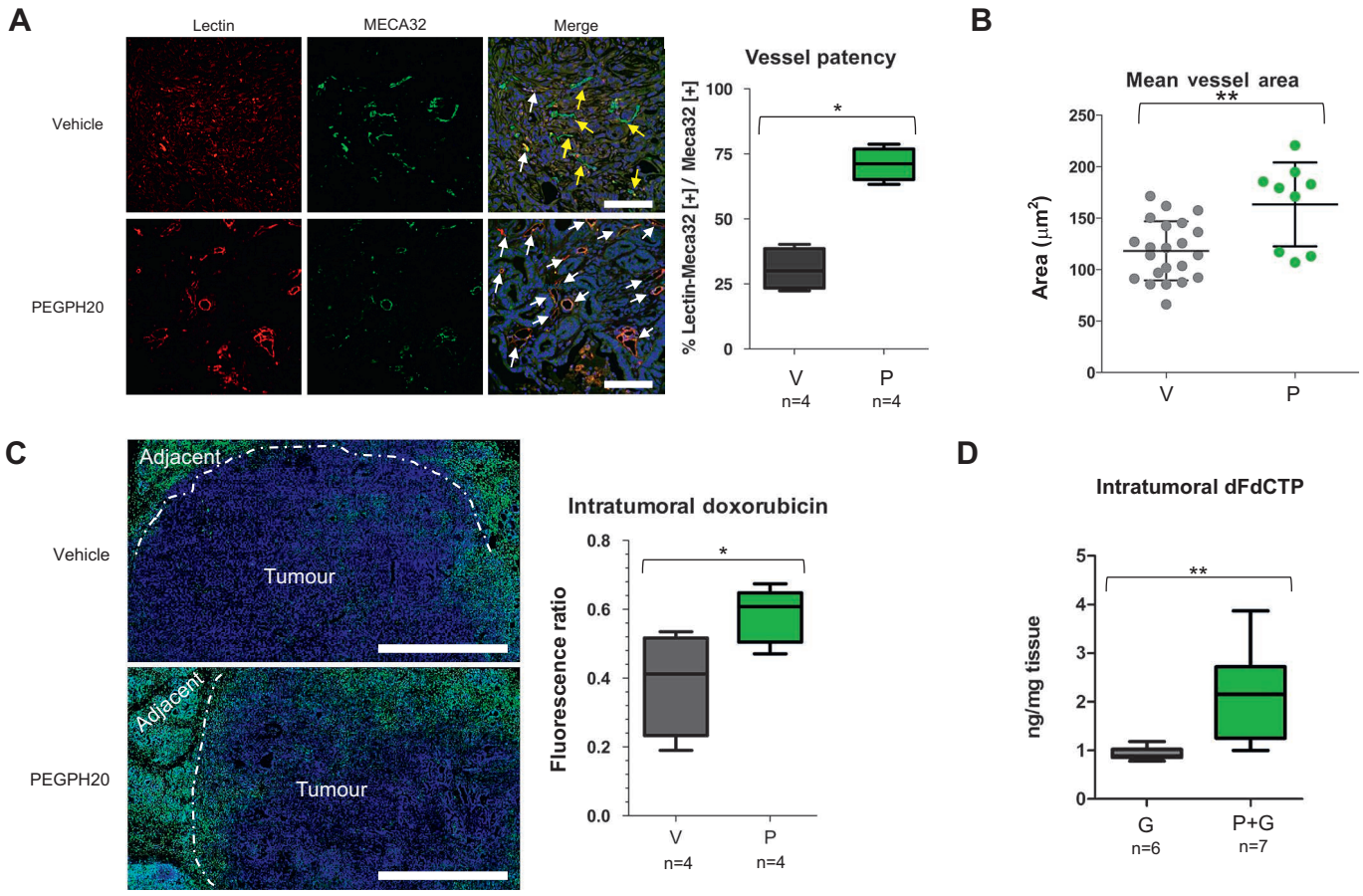

Figure 2 Depletion of hyaluronan improves vascular patency and increases chemotherapeutic delivery. (A) Fluorescence images of KPC tumours from vehicle-treated (top row, V) and PEGPH20-treated (bottom row, P) mice (n=4 animals in each cohort) terminally perfused with fluorescent biotinylated lectin (red). Total blood vessels are detected with MECA-32 antibody (green). White arrows denote functional vessels (red and green). Yellow arrows denote non-functional vessels (green only). Quantification of vessel patency indicates a significant increase in functional vessels after treatment with PEGPH20 (n=4 mice in each cohort, >100 vessels per mouse). Scale bar = 100 μm. Mann–Whitney U test, *p=0.0286. (B) Quantification of mean vessel area (in square micrometres) from anti-CD31-stained KPC tumours from vehicle-treated (V) or PEGPH20-treated (P) mice. A significant increase in mean vessel area is observed after treatment with PEGPH20, Mann–Whitney U test, **p=0.0085. (C) Fluorescent image of representative KPC tumour from vehicle-treated (top panel) and PEGPH20-treated (bottom panel) mice terminally perfused with autofluorescent small-molecule doxorubicin (pseudo-coloured green, n=4 mice in each cohort). Scale bar = 1 mm. Dotted white line denotes border between tumour core and adjacent diseased pancreatic tissue. Quantification of intratumoral doxorubicin as measured by fluorescence ratio in vehicle-treated (V) and PEGPH20-treated (P) KPC mice pancreatic ductal adenocarcinoma. Significant increase in intratumoral doxorubicin in PEGPH20-treated samples, Mann–Whitney U test, *p=0.0260. (D) Quantification of intratumoral gemcitabine triphosphate (dFdCTP), the active metabolite of gemcitabine (G), from vehicle- and PEGPH20-pretreated KPC mice. Significant increase in dFdCTP in PEGPH20-treated tumours, Mann–Whitney U test, **p=0.0053.

prior to incubation with bHABP (1:200 in 1% BSA) overnight at 4°C. Remaining steps were carried out using Vectastain Elite ABC kit Standard (Vector Laboratories) and DAB Peroxidase Substrate (Vector Laboratories), with haematoxylin counterstaining.

HA tissue microarray

Tissue microarrays were purchased from US Biomax Inc Rockville, MD, USA and stained with bHABP as described above. The slides were scanned at 20× magnification using Aperio ScanScope CS instrument and analysed in Spectrum automated slide analysis software (Aperio) using the positive pixel count algorithm. A ratio of strong positive stain area to the sum of total stained area was calculated and scored as 3+, 2+, 1+ or 0 when the ratio was more than 25%, 10%–25%, less than 10% or 0, respectively. See Supplemental Methods for further information.

Statistical analysis

GraphPad Prism 5 was used for all statistical analyses. The log-rank test was performed on the Kaplan–Meier survival curves, and the Mann–Whitney U test was performed for all other analyses.

RESULTS

HA accumulates in PDA and may be rapidly and sustainably degraded by PEGPH20

Using a modified histochemical method with bHABP and computer-assisted analysis, we examined the HA content in 204 normal and 1130 malignant human tissue samples. While a minority of normal epithelia demonstrated 1+ staining, HA was more frequently and abundantly detected in epithelial malignancies (table 1). Human PDA had the highest incidence of detectable HA content, and the majority of PDA samples was scored 2+ (figure 1A and data not shown). Notably, HA staining was predominantly associated with the desmoplastic stroma rather than with tumour cells. These histopathological observations were recapitulated in the tumours of KPC mice, where 2+ HA staining was observed in the stroma of most ductal tumours (figure 1B). This confirmed the suitability of the

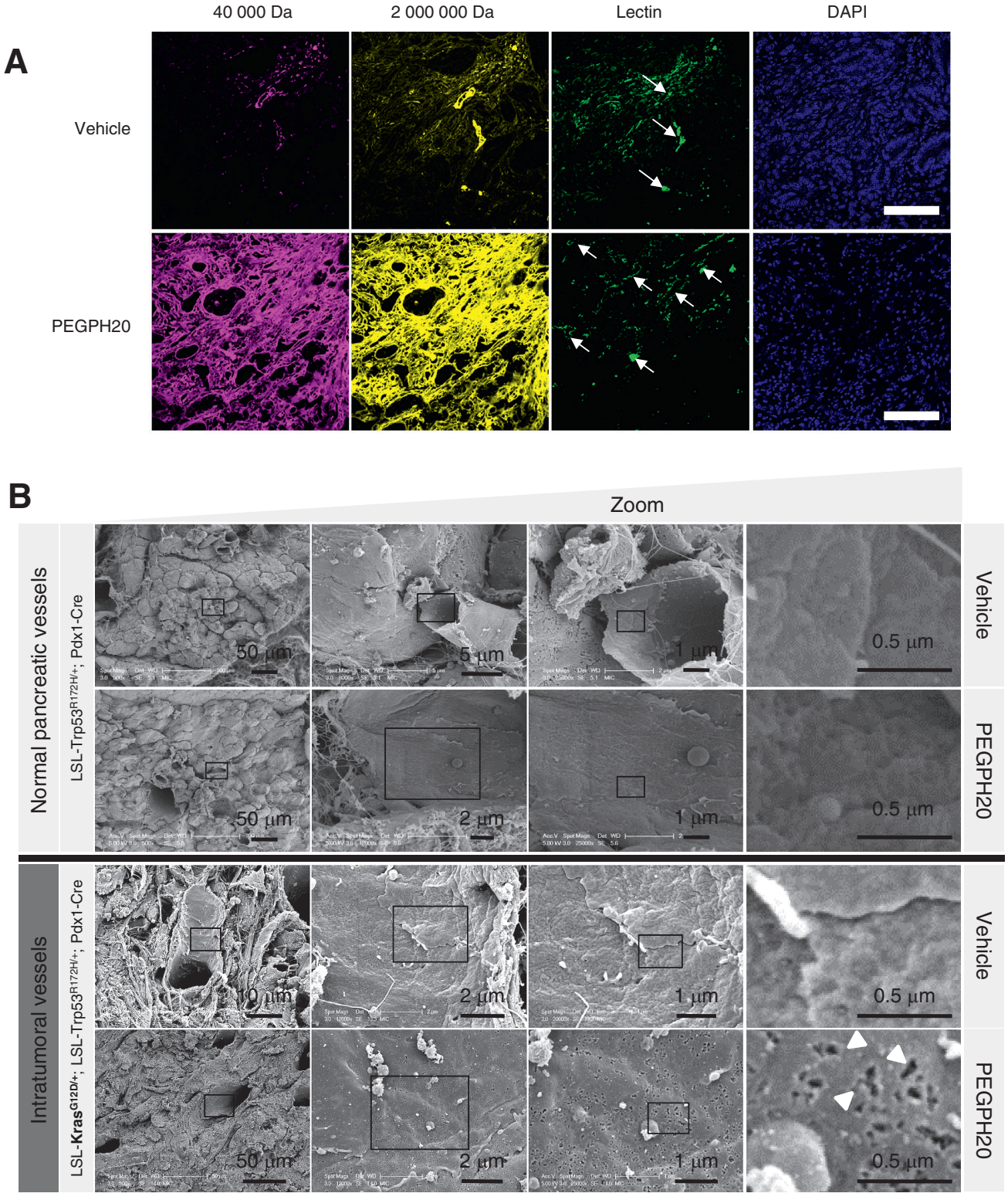

Figure 3 Depletion of hyaluronan increases macromolecular permeability and induces ultrastructural changes in tumour endothelia. (A) Representative fluorescent images of KPC tumour from vehicle-treated (top panel) and PEGPH20-treated (bottom panel) mice (n=4 mice for each cohort). Mice terminally treated with either low (40 kDa) or high (2 MDa) molecular weight dextrans with biotinylated lectin demonstrate a considerable increase in stromal and vessel permeability at the tumour core in PEGPH20-treated tumours. Arrows denote functional vessels in the field. Scale bar = 500 µm. (B) Scanning electron microscopy images of pancreatic blood vessels in PC (*LSL-Trp53$^{R172H/+}$;Pdx-1-Cre*) (upper two panels) and KPC (*LSL-Kras$^{G12D/+}$;LSL-Trp53$^{R172H/+}$;Pdx-1-Cre*) (lower two panels) mice following treatment with either vehicle or PEGPH20 (n=4 mice for each cohort) reveal endothelial fenestrations (white arrowheads) only in PEGPH20-treated KPC mice. (C) Quantification of density of fenestrae in intratumoral KPC blood vessels (n=3 mice for each cohort, four random vessels per mouse) revealed a significant increase following treatment with PEGPH20 (***p<0.0001). (D) Representative transmission electron micrographs from vehicle-treated (left panels) and PEGPH20-treated (right panels) tumours (n=4 mice for each cohort). Vehicle-treated tumours demonstrate juxtaposed endothelial cell membranes (red arrowheads), while prominent interendothelial gaps are present following treatment with PEGPH20 (designated by white diamonds, endothelial cell membranes denoted by blue arrowheads).

Figure 3 Continued

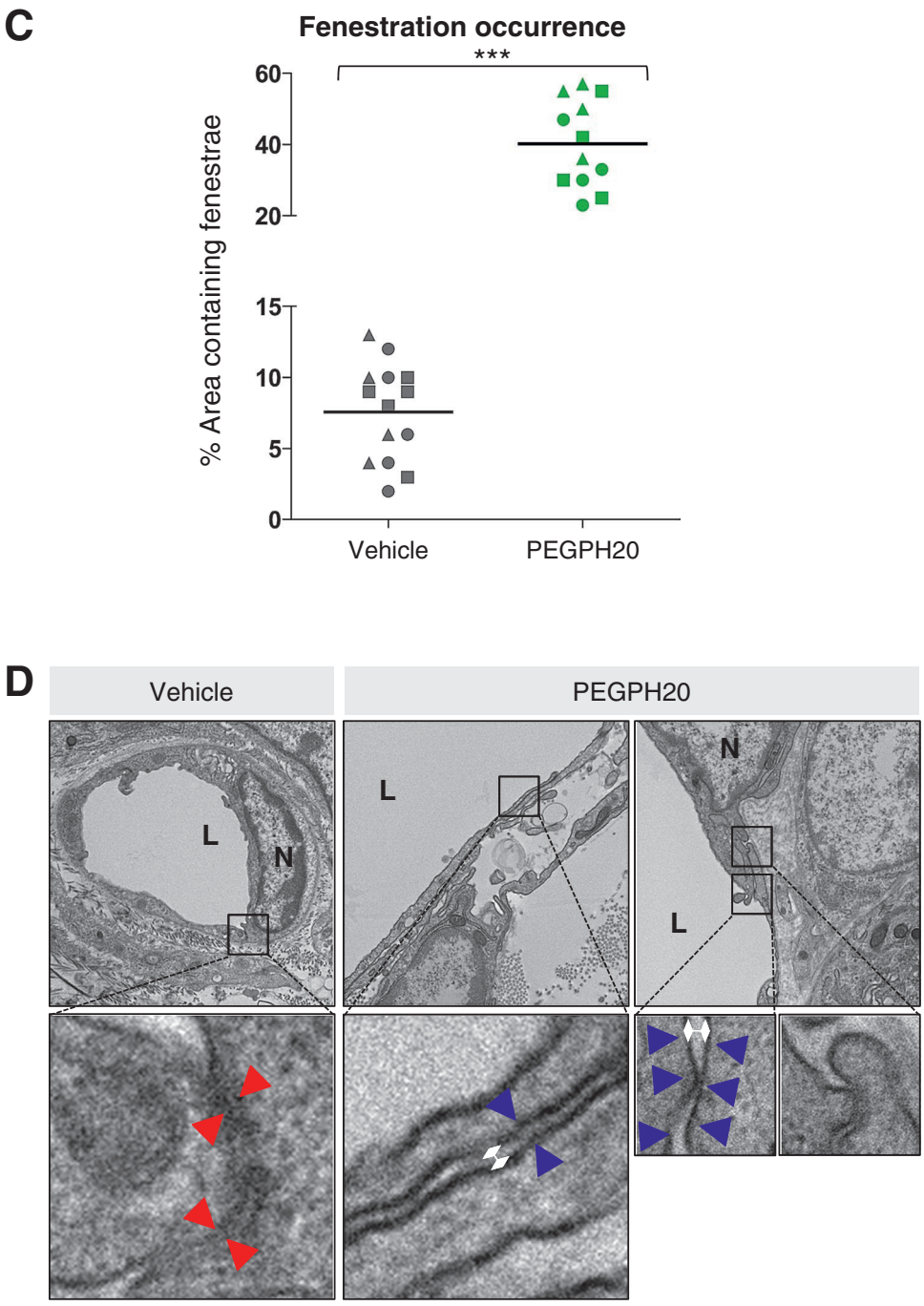

GEMM in determining HA's role in PDA structure and vascular function.

To determine whether HA could be depleted from primary pancreatic tumours, PEGPH20 was intravenously administered to KPC mice and tumours collected over a 3-day time course. A single dose of PEGPH20 at 4.5 mg/kg depleted intratumoral HA in a heterogeneous pattern within hours of administration, with little detectable HA remaining up to 72 h later (figure 1B).

Depletion of HA improves vascular patency and increases chemotherapeutic delivery

Consistent with previous reports,[7 8] less than one-third of the untreated KPC tumour vasculature is patent as delineated by *Lycopersicon esculentum* lectin perfusion (figure 2A). To evaluate vascular patency following complete depletion of HA, KPC mice were treated for 3 days with PEGPH20 prior to lectin perfusion and were killed. The hyaluronidase regimen resulted in an increased patency of the tumour vasculature (70% vs 30%, p=0.0286, figure 2A). Moreover, the majority of intratumoral vessels were noted to be prominently open, and, when measured, the mean vessel luminal area was found to be significantly increased (p=0.0085, figure 2B). Since treatment with PEGPH20 did not affect mean vessel density (figure S1), we reasoned that any increased perfusion could be attributed to decompression of existing intratumoral vessels.

We asked if vascular re-expansion might translate to an improvement in drug delivery. Exploiting the autofluorescence of anthracyclines, a significant increase in tumorous doxorubicin uptake was detected following pretreatment with the hyaluronidase (p=0.026, figure 2C). Similarly, mice receiving gemcitabine after a single dose of PEGPH20 demonstrated

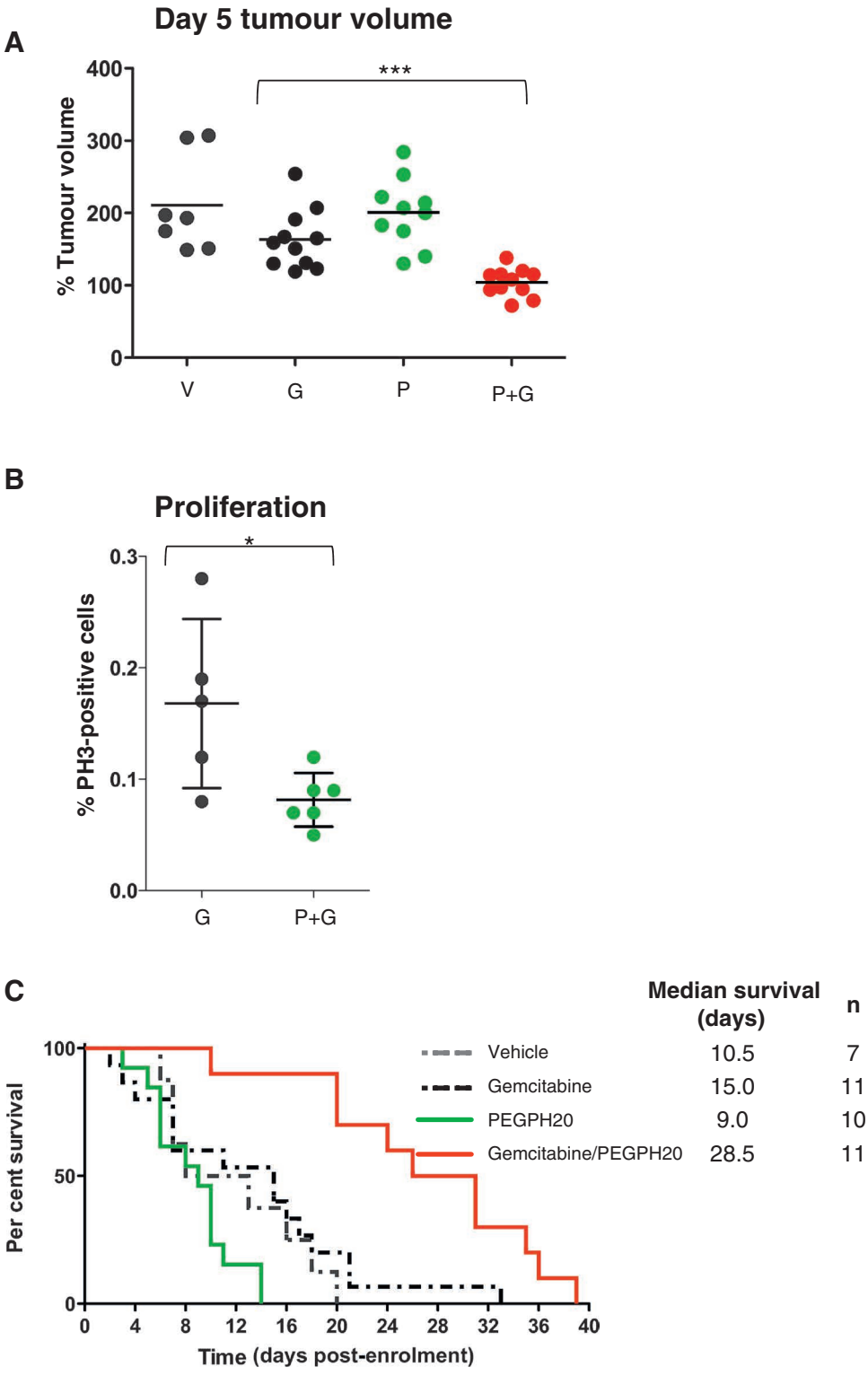

Figure 4 Combination therapy with PEGPH20 and gemcitabine inhibits tumour growth and significantly extends survival. (A) Tumour volume measurements from mice treated for 5 days with vehicle (V) (n=7), gemcitabine (G) (n=11), PEGPH20 (P) (n=10) and gemcitabine/PEGPH20 combination (P+G) (n=11) demonstrate cytostasis only in response to gemcitabine/PEGPH20 combination therapy. (B) Proliferation of pancreatic tumour cells in response to PEGPH20 treatment. A significant decrease in pancreatic tumour cell proliferation is observed 5 days after treatment with PEGPH20 and gemcitabine compared with gemcitabine alone. Mann–Whitney U test, *p=0.0432. (C) Kaplan–Meier survival curve for vehicle-treated (n=8, grey dotted line), gemcitabine-treated (n=15, black dotted line), PEGPH20-treated (n=12, green line) and gemcitabine/PEGPH20-treated (n=10, red line) KPC cohorts. A significant increase in survival was observed in gemcitabine/PEGPH20-treated mice relative to the gemcitabine-treated cohort. Log-rank ***p=0.0002, HR 0.06794. PH3, phospho-histone H3.

significantly increased intratumoral dFdCTP concentrations when compared with vehicle-pretreated counterparts (p=0.0053, figure 2D). Of note, PEGPH20 did not alter the plasma pharmacokinetic properties of gemcitabine in control mice (figure S2).

Depletion of HA increases macromolecular permeability and induces ultrastructural changes in tumour endothelia

To further characterise the KPC vasculature following HA depletion, fluorophore-conjugated high-molecular-weight dextrans (40 kDa and 2 MDa) were infused 30 min prior to tissue collection.[26] Dextran extravasation was minimal in untreated tumour tissue but increased dramatically following PEGPH20 treatment (figure 3A). Notably, macromolecular penetration was not improved in any healthy tissues tested (figure S3), even among those of high HA content such as cardiac muscle, suggestive of selective permeabilisation of the tumour vasculature.

The rapid and extensive intratumoral accumulation of 2 MDa dextran after PEGPH20 administration was unexpected, given

its large Stoke's radius. This prompted an examination of the tumour endothelial ultrastructure for vascular integrity and markers of induced hyperpermeability, which include fenestrae and intercellular gaps.[27–29] Notably, scanning electron microscopy revealed few fenestrations in the untreated tumour, comparable to endothelia in the healthy pancreata of control mice (figure 3B). Moreover, treatment-naive vasculature showed intact interendothelial junctions by transmission electron microscopy (figure 3D). By contrast, PEGPH20 induced a significant increase in fenestrae ($p<0.0001$, figure 3B,C) and more prominent interendothelial gaps (figure 3D), a hyperpermeability-associated phenotype reminiscent of VEGF-activated vasculature.[27–29]

Combination therapy with PEGPH20 and gemcitabine inhibits tumour growth and significantly extends survival

Given the improvement in pharmacodelivery, we evaluated whether PEGPH20 provided any therapeutic benefit to KPC mice either alone or in combination with gemcitabine. While gemcitabine monotherapy decreased tumour growth only modestly, the combination of PEGPH20 and gemcitabine significantly inhibited growth over 5 days of treatment ($p<0.001$, figure 4A). During the same period, PEGPH20 monotherapy had no effect on tumour growth (figure 4A). Growth inhibition was accompanied by a decrease in intratumoral proliferation as assessed by phospho-histone H3 staining ($p=0.043$, figure 4B).

To determine whether these findings impacted upon the lethality of PDA, KPC mice were subsequently treated for an extended period with each agent as monotherapy, with a vehicle or with the gemcitabine/PEGPH20 combination. Similar to the 5-day analysis, treatment with PEGPH20 or gemcitabine alone had insignificant effects on the survival of KPC mice in comparison to vehicle-treated mice (figure 4C). However, extended treatment with the gemcitabine/PEGPH20 combination significantly improved median survival over gemcitabine monotherapy (28.5 vs 15 days, $p=0.002$, figure 4C). Most mice in the gemcitabine/PEGPH20 combination cohort experienced stable tumour growth (figure S4) and hyaluronidase activity persisted up to study end point (figure S5).

DISCUSSION

We recently proposed that microenvironmental impairment in drug delivery may contribute towards the intrinsic chemoresistance of pancreatic cancer and used the Smoothened inhibitor IPI-926 to augment the response to gemcitabine in KPC mice.[7] However, since hedgehog signalling is implicated in the survival and propagation of stem-like cancer cells and cancer-associated fibroblasts,[30–32] an additional antitumour effect by IPI-926 could not be excluded. The current study with PEGPH20 supports the hypothesis that improvement of pharmacodelivery through depletion of select stromal components may be sufficient for the therapeutic response previously reported.[7]

The scarcity of endothelial fenestrations and open interendothelial junctions in treatment-naive KPC tumours stands in contrast to observations in xenografts, allografts and some spontaneous tumour models. A defective endothelial monolayer, characterised by abundant diaphragmed fenestrae and intercellular openings, is associated with VEGF-induced hyperpermeability[27 28] and underlies the vascular leakiness seen in these models.[29 33] Since these ultrastructural changes may permit access to therapeutic agents,[29] their absence may contribute towards delivery inefficiency in the KPC tumour and explain the differential chemotherapeutic sensitivities between spontaneous tumours and other models.[7] Moreover, the observation points to relative inactivity of VEGF in the tumour and is suggestive of signalling antagonism from the abundant angiostatic factors in KPC stroma.[34] Such an antiangiogenic milieu is generated by complex tumour–fibroblast interactions in PDA[35] and is frequently absent or lost in the pathogenesis of other tumour models.[36] Furthermore, the persistence of negative regulators of angiogenesis would explain the hypovascular phenotype and the failure of anti-VEGF agents in human PDA and its GEMMs.[8 37–39]

The unanticipated induction of fenestrae and impairment of junctional integrity following PEGPH20 may reflect the role of HA signalling in maintaining the PDA intratumoral vascular endothelium in a quiescent state. HA has been shown to impart increased barrier integrity and resistance to lipopolysaccharide-induced hyperpermeability through CD44-dependent reorganisation of the endothelial actin cytoskeleton.[40] Consistent with this finding, disruption of the HA–CD44 interaction in vivo by systemic administration of an anti-CD44 monoclonal results in a rapid permeability increase.[41] The generation of low-molecular-weight HA fragments (including oligosaccharides) in large quantities from intratumoral HA could antagonise existing HA–CD44 interactions[15 42] and may explain for the tumour specificity of PEGPH20-induced hyperpermeability.

The ultrastructural changes and the vascular re-expansion from IFP reduction have a multiplicative effect on intratumoral diffusion and convection by increasing both components of the permeability-surface area product.[43] Furthermore, IFP reduction results in a favourable hydrostatic pressure gradient for convective solute delivery. The specificity of this effect to the tumour suggests utility as an adjunct to agents of larger hydrodynamic size, such as polymeric drugs, monoclonal antibodies and albumin conjugates. Nonetheless, as prior work in xenografts suggested monotherapy activity of PEGPH20,[20] we cannot exclude the possibility that HA depletion also sensitises neoplastic cells to gemcitabine toxicity by removing various survival cues. Finally, the synergism of PEGPH20 and gemcitabine demonstrated in this study is of immediate clinical significance and provides support for investigational trials with this therapeutic combination (NCT01453153).

Acknowledgements We thank the members of the Tuveson's laboratory for assistance and advice, and the animal care staff, histology and microscopy cores at Cambridge Research Institute, specifically F Connor, P Mackin, L Young, L Shelbourne, S Kupczak, M Cronshaw, Y Cheng, M Pryor, E Pryor, B Wilson, L McDuffus, J Atkinson, J Miller, W Howat and S Reichelt. We also thank E Miklejewska for assisting with SEM.

Contributors MAJ, DSC, AN, NC, CF, TN, MPL and KKF performed in vivo experiments. MAJ, DSC, MEC, HIZ, AK, PJ and JNS performed microscopy experiments. MAJ, DSC, AN, TEB, NC, KKF, DCM, CBT and DIJ performed pharmacology studies. MAJ, DSC, AN, HMS, GIF and DT designed the study and co-wrote the manuscript, and all authors commented on it.

Funding This research was supported by the University of Cambridge and Cancer Research UK, the Li Ka Shing Foundation and Hutchison Whampoa Limited, the National Institute for Health Research Cambridge Biomedical Research Centre and the European Commission Seventh Framework Programme (FP7 Health 2010 2.4.1-6, contract number 256974). AN was supported by the Mildred Scheel Postdoctoral Fellowship by the Deutsche Krebshilfe. NC was supported by a Cancer Research UK Clinician Fellowship. CF was supported by the EMBO long-term fellowship and by a Marie Curie Intra European Fellowship within the Seventh European Community Framework Programme. MPL has received a Dutch Cancer Foundation Fellowship grant (UU2008-4380) to support this work. DT and DIJ are group leaders in the Cancer Research UK Cambridge Research Institute.

Competing interests DCM, CBT, PJ, AK, HMS and GIF are employees of Halozyme.

Provenance and peer review Not commissioned; internally peer reviewed.

REFERENCES

1. **Vincent A,** Herman J, Schulick R, *et al*. Pancreatic cancer. *Lancet* 2011;**378**:607—20.
2. **Burris HA 3rd,** Moore MJ, Andersen J, *et al*. Improvements in survival and clinical benefit with gemcitabine as first-line therapy for patients with advanced pancreas cancer: a randomized trial. *J Clin Oncol* 1997;**15**:2403—13.
3. **Sultana A,** Smith CT, Cunningham D, *et al*. Meta-analyses of chemotherapy for locally advanced and metastatic pancreatic cancer. *J Clin Oncol* 2007;**25**:2607—15.
4. **Aguirre AJ,** Bardeesy N, Sinha M, *et al*. Activated Kras and Ink4a/Arf deficiency cooperate to produce metastatic pancreatic ductal adenocarcinoma. *Genes Dev* 2003;**17**:3112—26.
5. **Hingorani SR,** Wang L, Multani AS, *et al*. Trp53R172H and KrasG12D cooperate to promote chromosomal instability and widely metastatic pancreatic ductal adenocarcinoma in mice. *Cancer Cell* 2005;**7**:469—83.
6. **Bardeesy N,** Aguirre AJ, Chu GC, *et al*. Both p16(Ink4a) and the p19(Arf)-p53 pathway constrain progression of pancreatic adenocarcinoma in the mouse. *Proc Natl Acad Sci USA* 2006;**103**:5947—52.
7. **Olive KP,** Jacobetz MA, Davidson CJ, *et al*. Inhibition of Hedgehog signaling enhances delivery of chemotherapy in a mouse model of pancreatic cancer. *Science* 2009;**324**:1457—61.
8. **Olson P,** Chu GC, Perry SR, *et al*. Imaging guided trials of the angiogenesis inhibitor sunitinib in mouse models predict efficacy in pancreatic neuroendocrine but not ductal carcinoma. *Proc Natl Acad Sci USA* 2011;**108**:E1275—84.
9. **Komar G,** Kauhanen S, Liukko K, *et al*. Decreased blood flow with increased metabolic activity: a novel sign of pancreatic tumor aggressiveness. *Clin Cancer Res* 2009;**15**:5511—17.
10. **Young JS,** Lumsden CE, Stalker AL. The significance of the tissue pressure of normal testicular and of neoplastic (Brown-Pearce carcinoma) tissue in the rabbit. *J Pathol Bacteriol* 1950;**62**:313—33.
11. **Goldacre RJ,** Sylven B. On the access of blood-borne dyes to various tumour regions. *Br J Cancer* 1962;**16**:306—22.
12. **Stohrer M,** Boucher Y, Stangassinger M, *et al*. Oncotic pressure in solid tumors is elevated. *Cancer Res* 2000;**60**:4251—5.
13. **Heldin CH,** Rubin K, Pietras K, *et al*. High interstitial fluid pressure—an obstacle in cancer therapy. *Nat Rev Cancer* 2004;**4**:806—13.
14. **Jain RK.** Normalization of tumor vasculature: an emerging concept in antiangiogenic therapy. *Science* 2005;**307**:58—62.
15. **Toole BP,** Slomiany MG. Hyaluronan: a constitutive regulator of chemoresistance and malignancy in cancer cells. *Semin Cancer Biol* 2008;**18**:244—50.
16. **Chahine NO,** Chen FH, Hung CT, *et al*. Direct measurement of osmotic pressure of glycosaminoglycan solutions by membrane osmometry at room temperature. *Biophys J* 2005;**89**:1543—50.
17. **Beckenlehner K,** Bannke S, Spruss T, *et al*. Hyaluronidase enhances the activity of adriamycin in breast cancer models in vitro and in vivo. *J Cancer Res Clin Oncol* 1992;**118**:591—6.
18. **Brekken C,** de Lange Davies C. Hyaluronidase reduces the interstitial fluid pressure in solid tumours in a non-linear concentration-dependent manner. *Cancer Lett* 1998;**131**:65—70.
19. **Whatcott CJ,** Han H, Posner RG, *et al*. Targeting the tumor microenvironment in cancer: why hyaluronidase deserves a second look. *Cancer Discov* 2011;**1**:291—6.
20. **Thompson CB,** Shepard HM, O'Connor PM, *et al*. Enzymatic depletion of tumor hyaluronan induces antitumor responses in preclinical animal models. *Mol Cancer Ther* 2010;**9**:3052—64.
21. **Mahlbacher V,** Sewing A, Elsässer HP, *et al*. Hyaluronan is a secretory product of human pancreatic adenocarcinoma cells. *Eur J Cell Biol* 1992;**58**:28—34.
22. **Theocharis AD,** Tsara ME, Papageorgacopoulou N, *et al*. Pancreatic carcinoma is characterized by elevated content of hyaluronan and chondroitin sulfate with altered disaccharide composition. *Biochim Biophys Acta* 2000;**1502**:201—6.
23. **Fries H,** Elsässer HP, Mahlbacher V, *et al*. Localisation of hyaluronate (HA) in primary tumors and nude mouse xenografts of human pancreatic carcinomas using a biotinylated HA-binding protein. *Virchows Arch* 1994;**424**:7—12.
24. **Sironen RK,** Tammi M, Tammi R, *et al*. Hyaluronan in human malignancies. *Exp Cell Res* 2011;**317**:383—91.
25. **Bapiro TE,** Richards FM, Goldgraben MA, *et al*. A novel method for quantification of gemcitabine and its metabolites 2′,2′-difluorodeoxyuridine and gemcitabine triphosphate in tumour tissue by LC-MS/MS: comparison with (19)F NMR spectroscopy. *Cancer Chemother Pharmacol* 2011;**68**:1243—53.
26. **Dreher MR,** Liu W, Michelich CR, *et al*. Tumor vascular permeability, accumulation, and penetration of macromolecular drug carriers. *J Natl Cancer Inst* 2006;**98**:335—44.
27. **Roberts WG,** Palade GE. Increased microvascular permeability and endothelial fenestration induced by vascular endothelial growth factor. *J Cell Sci* 1995;**108**:2369—79.
28. **Roberts WG,** Palade GE. Neovasculature induced by vascular endothelial growth factor is fenestrated. *Cancer Res* 1997;**57**:765—72.
29. **Hashizume H,** Baluk P, Morikawa S, *et al*. Openings between defective endothelial cells explain tumor vessel leakiness. *Am J Pathol* 2000;**156**:1363—80.
30. **Mueller MT,** Hermann PC, Witthauer J, *et al*. Combined targeted treatment to eliminate tumorigenic cancer stem cells in human pancreatic cancer. *Gastroenterology* 2009;**137**:1102—13.
31. **Tian H,** Callahan CA, DuPree KJ, *et al*. Hedgehog signaling is restricted to the stromal compartment during pancreatic carcinogenesis. *Proc Natl Acad Sci USA* 2009;**106**:4254—9.
32. **Walter K,** Omura N, Hong SM, *et al*. Overexpression of smoothened activates the sonic hedgehog signaling pathway in pancreatic cancer-associated fibroblasts. *Clin Cancer Res* 2010;**16**:1781—9.
33. **Hobbs SK,** Monsky WL, Yuan F, *et al*. Regulation of transport pathways in tumor vessels: role of tumor type and microenvironment. *Proc Natl Acad Sci USA* 1998;**95**:4607—12.
34. **Kisker O,** Onizuka S, Banyard J, *et al*. Generation of multiple angiogenesis inhibitors by human pancreatic cancer. *Cancer Res* 2001;**61**:7298—304.
35. **Erkan M,** Reiser-Erkan C, Michalski CW, *et al*. Cancer-stellate cell interactions perpetuate the hypoxia-fibrosis cycle in pancreatic ductal adenocarcinoma. *Neoplasia* 2009;**11**:497—508.
36. **Xie L,** Duncan MB, Pahler J, *et al*. Counterbalancing angiogenic regulatory factors control the rate of cancer progression and survival in a stage-specific manner. *Proc Natl Acad Sci USA* 2011;**108**:9939—44.
37. **Kindler HL,** Niedzwiecki D, Hollis D, *et al*. Gemcitabine plus bevacizumab compared with gemcitabine plus placebo in patients with advanced pancreatic cancer: phase III trial of the Cancer and Leukemia Group B (CALGB 80303). *J Clin Oncol* 2010;**28**:3617—22.
38. **O'Reilly EM,** Niedzwiecki D, Hall M, *et al*. A Cancer and Leukemia Group B phase II study of sunitinib malate in patients with previously treated metastatic pancreatic adenocarcinoma (CALGB 80603). *Oncologist* 2010;**15**:1310—19.
39. **Kindler HL,** Ioka T, Richel DJ, *et al*. Axitinib plus gemcitabine versus placebo plus gemcitabine in patients with advanced pancreatic adenocarcinoma: a double-blind randomised phase 3 study. *Lancet Oncol* 2011;**12**:256—62.
40. **Singleton PA,** Mirzapoiazova T, Guo Y, *et al*. High-molecular-weight hyaluronan is a novel inhibitor of pulmonary vascular leakiness. *Am J Physiol Lung Cell Mol Physiol* 2010;**299**:L639—51.
41. **Tanaka Y,** Makiyama Y, Mitsui Y. Anti-CD44 monoclonal antibody (IM7) induces murine systemic shock mediated by platelet activating factor. *J Autoimmun* 2002;**18**:9—15.
42. **Lennon FE,** Singleton PA. Hyaluronan regulation of vascular integrity. *Am J Cardiovasc Dis* 2011;**1**:200—13.
43. **Jain RK,** Baxter LT. Mechanisms of heterogeneous distribution of monoclonal antibodies and other macromolecules in tumors: significance of elevated interstitial pressure. *Cancer Res* 1988;**48**:7022—32.